Cell Reports, Volume *33*

Supplemental Information

The Deubiquitinating Enzyme Ataxin-3 Regulates Ciliogenesis and Phagocytosis in the Retina

Vasileios Toulis, Sílvia García-Monclús, Carlos de la Peña-Ramírez, Rodrigo Arenas-Galnares, Josep F. Abril, Sokol V. Todi, Naheed Khan, Alejandro Garanto, Maria do Carmo Costa, and Gemma Marfany

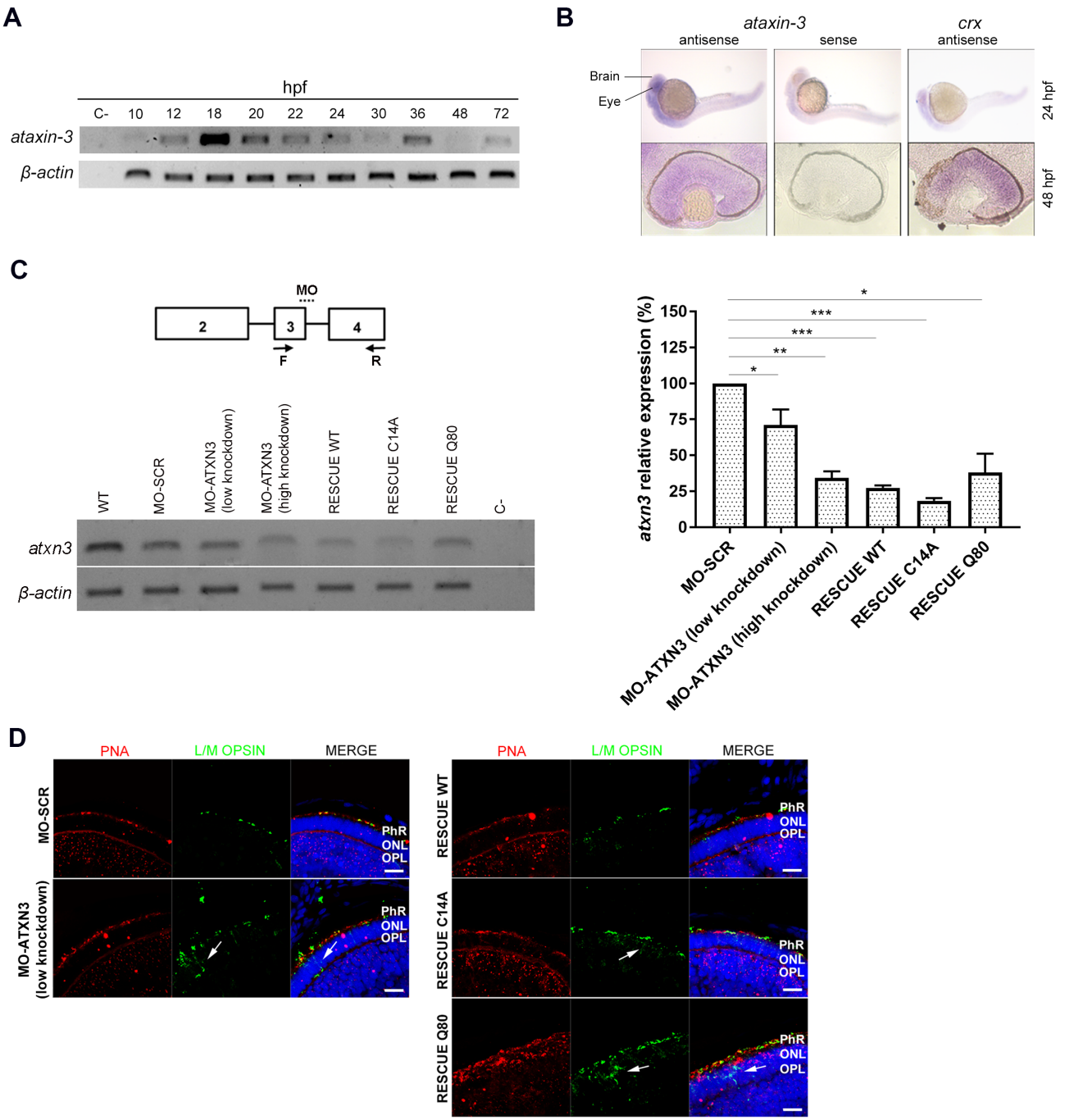

Figure S1. Retinal expression and morpholino-mediated knockdown of *atxn3* in zebrafish (Related to Figure 1). A, Expression of *atxn3* in zebrafish at relevant ocular developmental stages, from 10 to 72 hours post-fertilization (hpf) (Kimmel et al., 1995). The expression of *atxn3* reaches two peaks preceding the formation of relevant eye structures, at the 18-somite stage (18 hpf), when the developing zebrafish eyecup becomes thicker and at the prim-25 stage (36 hpf), when the eyecup begins to differentiate into the neural retina and retinal pigment epithelium. **B**, *In situ* hybridization of *atxn3* in the developing retina of whole embryos at 24 hpf (early differentiation of the retina and retinal pigment epithelium) and in embryonic retinas sections (48 hpf, generation of the neuronal retinal layers). *atxn3* transcript is detectable at 24 hpf in the anterior part of the embryo, more specifically in the eye and brain. At 48 hpf, the hybridization signal is observed throughout all the retinal tissue, particularly in regions that will later develop into the two plexiform layers. **C**, The antisense morpholino (dashed line in the diagram) targeting the donor splice site of exon 3 was designed to cause either intron 3 retention or exon 3 skipping. Morpholino-mediated knockdown of atxn3 was assessed by semi-quantitative RT-PCR of total RNA extracted from a pool of 10-12 injected embryos (at 72 hpf) for each condition (a representative agarose gel for one experiment is shown). The amplified fragment comprised exon 3 and 4 of *atxn3* (arrows F and R show the location of the primers). β-actin expression was used for normalization. Quantification of 3 independent experiments confirmed the gene knockdown (low or high in the different phenotypic groups) after morpholino injection and in rescue experiments. Note that the morpholino sequence and the primers for RT-PCR were specific for the zebrafish *atxn3* sequence and, therefore, did not target or amplify human *ATXN3* transcripts. Statistical significance analysis by the Wilcoxon signed-rank test (* $p<0.05$, ** $p<0.01$, *** $p<0.001$). **D**, Immunodetection of peanut agglutinin (PNA, red, cones) and L/M opsins (green) in

zebrafish embryo retinas shows mislocalization of opsins (white arrows point to ectopic cone opsin detection in the cone nuclei at ONL and cone axons in the OPL) in knockdown MO-ATXN3 compared to control MO-SCR retinas. This altered cone phenotype in MO-ATXN3 morphants is successfully rescued with co-injection of ATXN3 WT, but not with C14A and Q80 mutant mRNAs. Scale bar, 10 μm. All images are representative of 3-4 retinal cryosections of embryos at 72 hpf per group (independent replicates). Nuclei were counterstained with DAPI (blueMO-ATXN3: embryos injected with a morpholino targeting *atxn3*; MO-SCR: scrambled control morpholino; RESCUE: phenotypic rescue of embryos co-injected with *atxn3* morpholinos –to knockdown the endogenous zebrafish gene– and mRNAs from either WT (normal Q22), expanded Q80 or catalytically inactive C14A ATXN3 alleles. PhR- Photoreceptor layer; ONL- outer nuclear layer; OPL- outer plexiform layer.

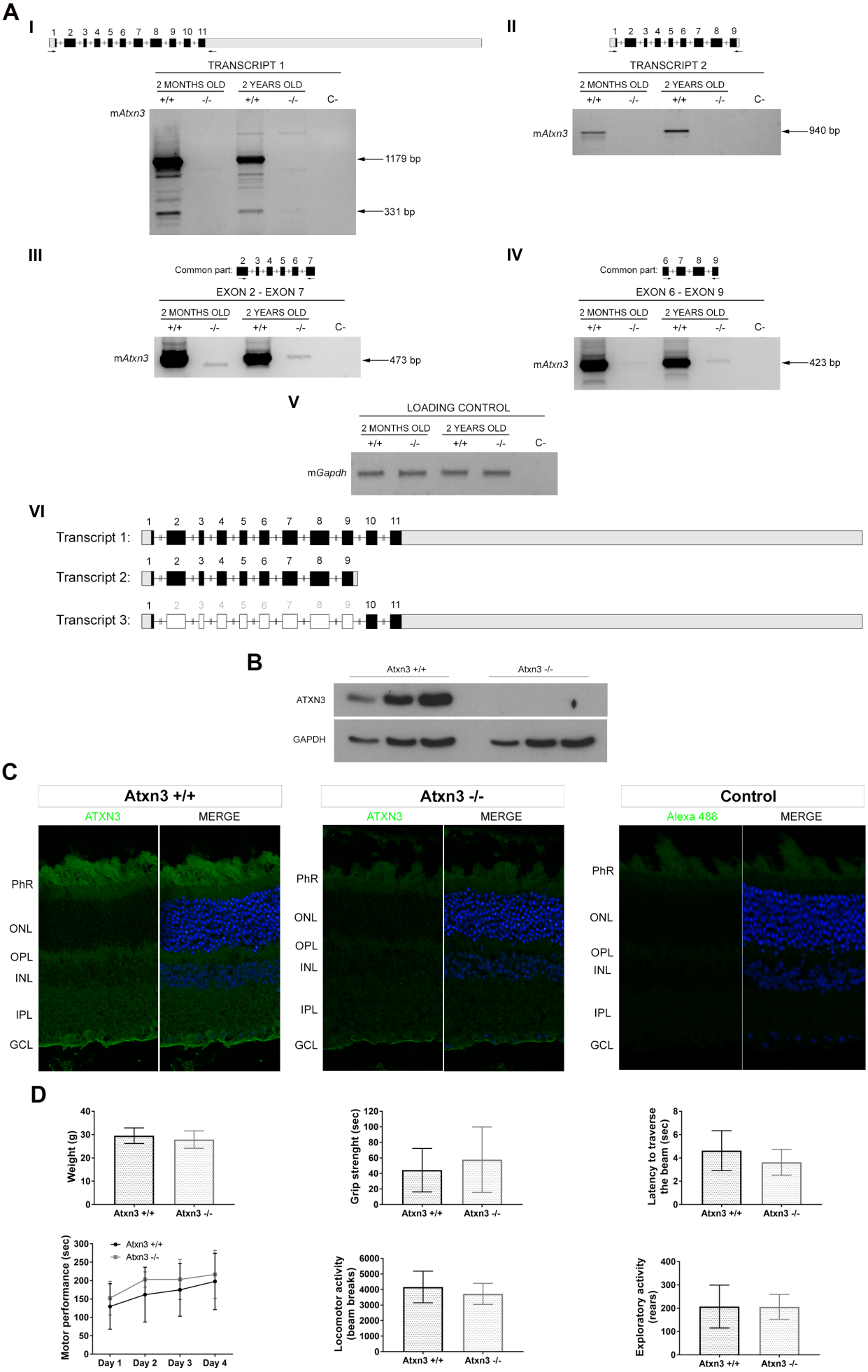

Figure S2. Molecular and behavioral characterization of *Atxn3* KO mice. (Related to Figure 2). A, Expression levels of the two mouse *Atxn3* transcripts detected by semi-quantitative PCR in *Atxn3* WT and KO

retinas. Primers (black arrows) are located either in specific sequences of the 5′UTR and 3′UTR to detect transcript 1 (I) and transcript 2 (II), or in the common region (III and IV). An almost complete reduction of *Atxn3* mRNA expression was observed. The band of 331 bp in the WT retina samples (I) corresponds to a new and out-of-frame transcript that shares the 5′ and 3′UTRs with transcript 1. All other bands in this figure were discarded as being *Atxn3* products after purification and Sanger sequencing. (V) *Gapdh* expression was used for normalization. (VI) Diagram depicting the exon structure of the three transcripts detected in *Atxn3* WT retinas. **B,** Western-blot analysis using anti-MJD of three WT and three *Atxn3* KO retinas from individual mice revealed ablation of ATXN3 levels in the KO. GAPDH was used for normalization. **C,** Immunofluorescent detection in *Atxn3* WT and KO retina cryosections showed higher expression levels of ATXN3 (in green) in photoreceptor and ganglion cell layers. Negative control with only the secondary antibody is also shown. Nuclei were counterstained with DAPI (blue). PhR, photoreceptors; ONL, outer nuclear layer; OPL, outer plexiform layer; INL, inner nuclear layer; IPL, inner plexiform layer; GCL, ganglion cell layer. **D,** *Atxn3*-/- mice show normal locomotor and exploratory behavior compared to *Atxn3*+/+ controls . No differences in the body weight were observed between *Atxn3*+/+ and *Atxn3*-/- mice. Normal grip strength of *Atxn3-/-* mice, manifested by the latency to fall from an inverted grid cage (bars represent the mean time ± SD). Normal gait, balance, and locomotor function of *Atxn3-/-* mice on 5-mm-squared beam walking test, manifested by the latency to traverse the beam (bars represent the mean of two consecutive trials on day 4 of testing ± SD), and the rotarod apparatus, measuring the latency to fall on a 4-40 rpm acceleration rod (lines represent the mean time ± SD of the two trials for four consecutive days). *Atxn3*-/- mice display normal locomotor (beam breaks, exploratory activity and number of rears on the open-field test for 30 minutes (bars represent mean ± SD). Number of mice per group ranged from N = 5-8.

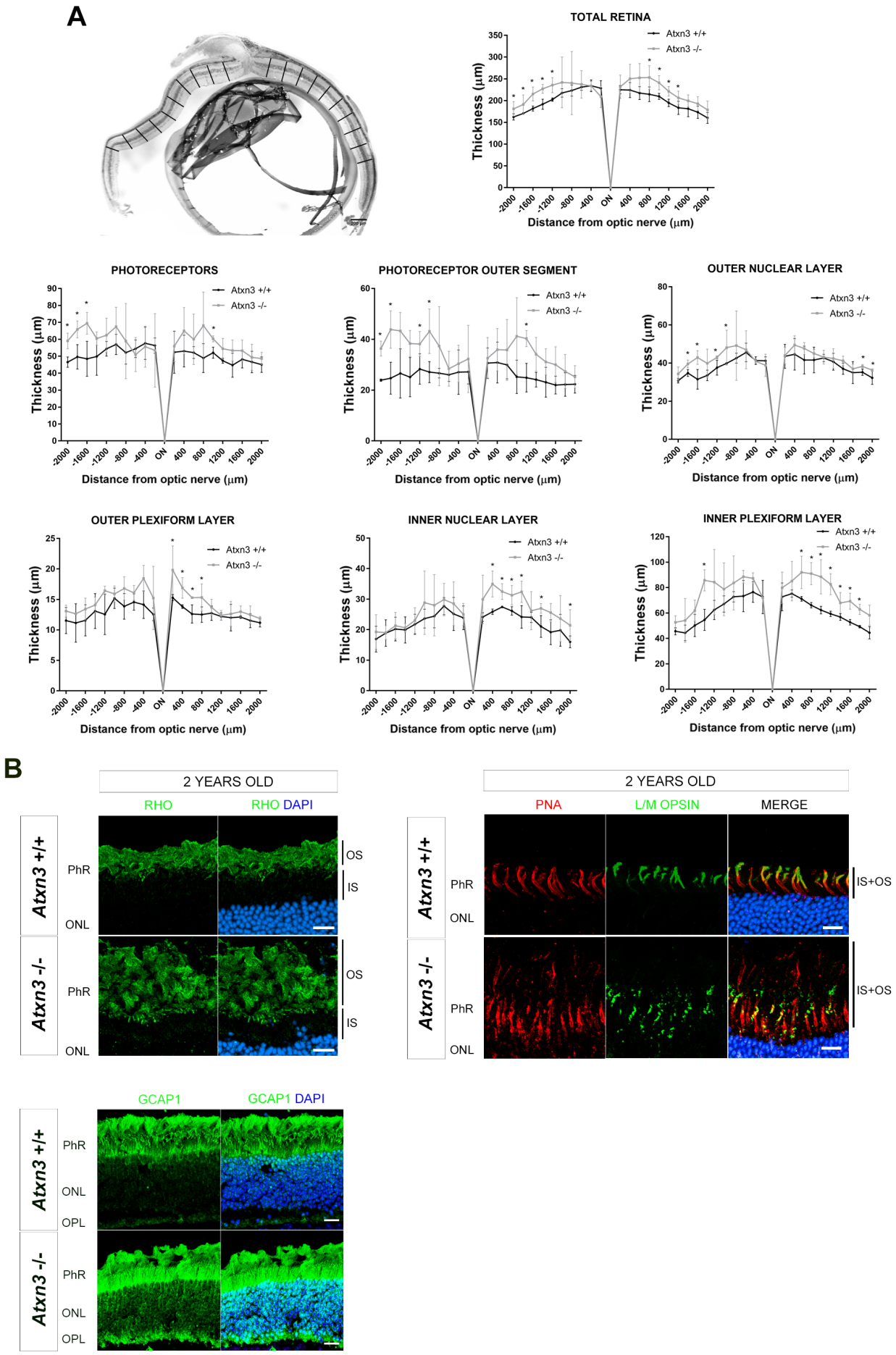

Figure S4. Morphometric analysis and immunodetection on 2 year-old retinal sections reveal an enlargement of the retinal layers in the retinas of *Atxn3* KO mice due to an elongation of photoreceptor outer segment (Related to Figure 2). **A**, Morphometric measurements were performed in central retina slides

(see representative image) containing the optic nerve. Retinal thickness was measured at 200 µm intervals (vertical black lines) covering the whole length of the central retina. Atxn3 KO (Atxn3 -/-) retinas showed an enlargement not only in the total retina thickness, but also particularly in the photoreceptor and inner plexiform layers, compared to the wild-type retinas (Atxn3 +/+). Mean values and standard deviation were obtained from three littermate mice per genotype. Statistical significance by the Mann-Whitney test (* $p<0.05$). B, Confocal microscopy shows elongation of photoreceptor outer segments (Os) and cone opsin mislocalisation (similar results as main Fig.2 but in 2 year-old mouse retinas) as observed by immunodetection of rod rhodopsin (RHO, green) on retinal cryosections from WT (Atxn3 +/+) and KO (Atxn3 -/-). Besides, immunodetection of L/M Opsins (green) and peanut agglutinin (PNA, red) shows mislocalisation of cone opsins in the enlarged OS, extending also into the inner segment (IS), in Atxn3 KO cones (vertical black line at the right panels) compared to WT controls. Immunofluorescent detection of GCAP1 (green) and PNA (red, labelling cones) in mouse retinal cryosections shows GCAP1 retention in the inner segment of cones (left panels) and GCAP1 mislocalisation in the ONL and OPL of the photoreceptors of Atxn3 KO compared to WT retinas. All the retinas were extracted at the same time point of the day for comparison, as many phototransduction proteins shift their localisation according to the circadian light-dark cycle. Nuclei were counterstained with DAPI (blue). Scale bar, 10 µm. PhR, photoreceptors; ONL, outer nuclear layer; OPL, outer plexiform layer.

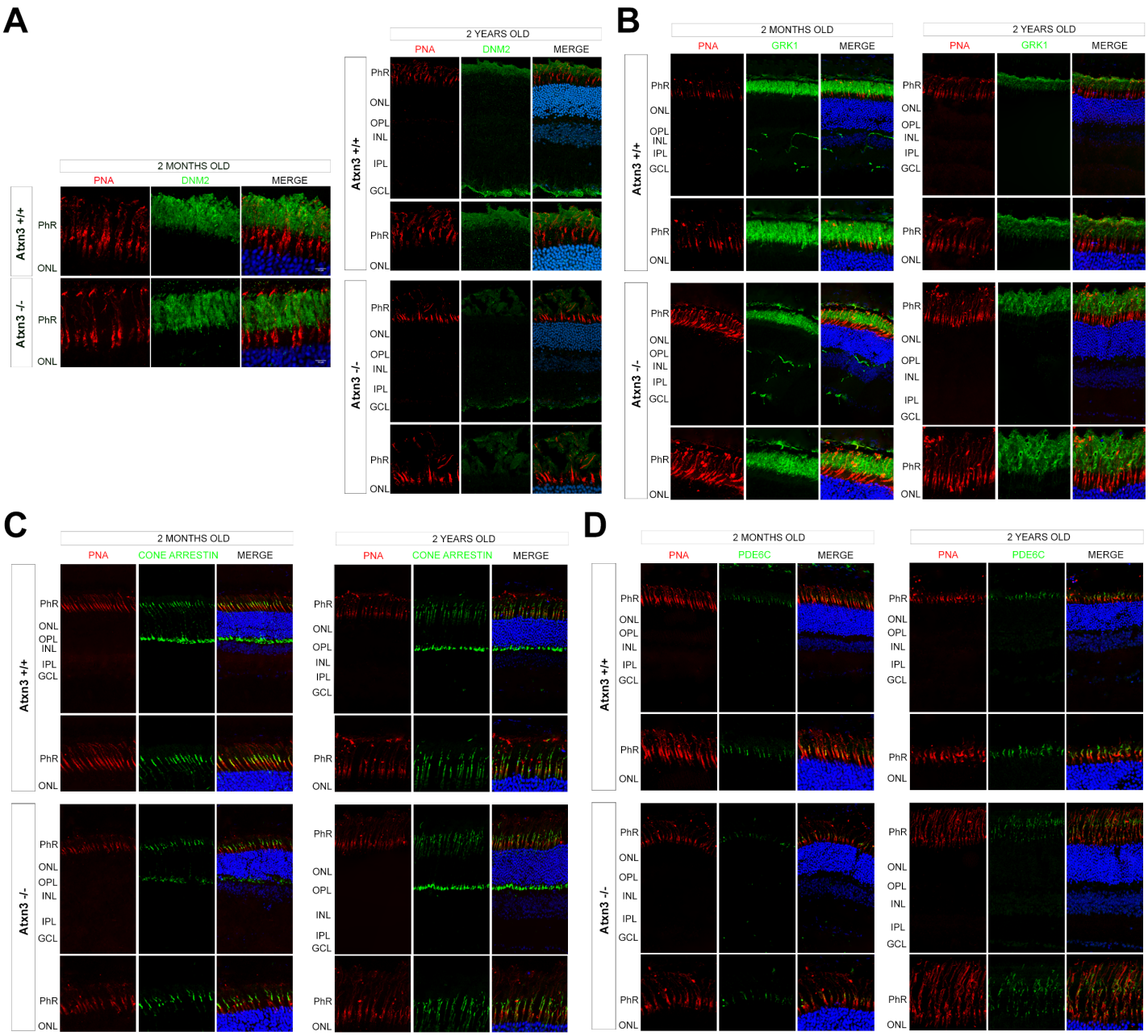

Figure S4. Normal localization of several proteins involved in the phototransduction cascade in *Atxn3 -/-* KO photoreceptors in young and aged mice. (Related to Figure 2). Immunofluorescent detection in WT and KO retina cryosections from 2 month- and 2 year-old mice of **A,** DNM2 (green), **B,** GRK1 (green), **C,** Cone arrestin (green) and **D,** PDE6C (green). In all sections, PNA (peanut agglutinin, in red) labeled cone membrane, and nuclei were counterstained with DAPI (blue). PhR, photoreceptors; ONL, outer nuclear layer; OPL, outer plexiform layer; INL, inner nuclear layer; IPL, inner plexiform layer; GCL, ganglion cell layer.

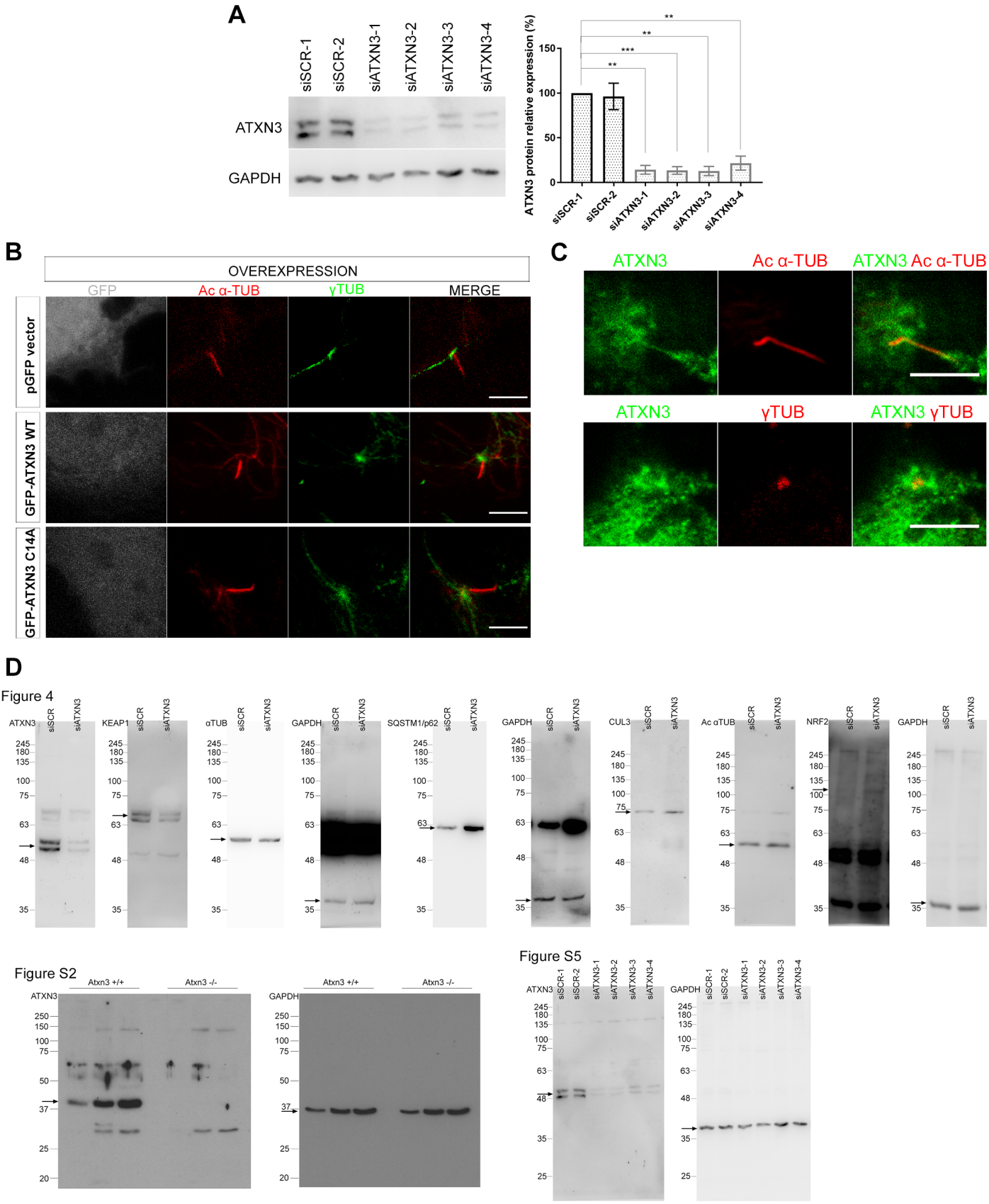

Figure S5. Knockdown of *ATXN3* in siATXN3-treated cells, localization of ATXN3 in ciliary compartments in ARPE-19 cells, including uncropped western blots. (Related to Figures 3, 4, S2 and S5). A, Immunodetection of human ARPE-19 cells transfected with two different scrambled siRNAs (siSCR) or four different siRNAs targeting the endogenous *ATXN3* (siATXN3). The two bands immunodetected for ATXN3 correspond to two different alleles bearing different CAG repeat sizes within the normal range. Depletion of more than 85% of ATXN3 levels was achieved using siATXN3-1, siATXN3-2 and siATXN3-3. Since the results were consistent and repetitive (at least 3 or more independent replicates), we decided to use siATXN3-2 theretofore. Statistical significance analysis by One-sample T-

test or Wilcoxon signed-rank test. * P<0.05, ** P<0.01, *** P<0.001. **B,** Immunodetection of acetylated-α-tubulin (red) and γ-tubulin (green) of starved human ARPE-19 overexpressing either GFP-ATXN3 WT Q22, GFP-ATXN3 C14A mutant, or the pEGFP empty vector (negative control). Scale bar, 5 μm. These are the same images as in main Figure 3, but showing that transfected cells are GFP-positive (grey). **C**, Comparative localization of single confocal planes showing the endogenous ATXN3 (in green) in the ciliary elements, axoneme and basal body, as detected by acetylated-α-tubulin and γ-tubulin (all in red), showing that ATN3 localizes at the ciliary compartments to some extent. Scale bar 5 μm. **D**, Uncropped blots of all the western detections in Figures 4, S2 and in this figure S5 (as indicated). Note that some of the blots first used to immunodetect the protein of interest (size indicated by a black arrow) have been later reused to detect control proteins.